Supporting Information

Niedermeyer et al. 10.1073/pnas.1323585111

SI Text

Regional Setting

Northwest Sumatra is located within the equatorial rainfall regime, which is characterized by high amounts of rainfall throughout the year and no dry season (1). Depending on the seasonal position of the Intertropical Convergence Zone (ITCZ), rainfall delivered by the maritime trade winds originates from the converging branches of either the northern or the southern Hadley cell (Fig. S1), resulting in two rainfall maxima during spring and fall. As the contribution of each season to the total amount of rainfall does not differ significantly, Northwest Sumatra is not attributed to the realms of the Australian–Indonesian or Asian monsoons (2, 3). With increasing distance from the equator, however, seasonal changes in the amount of rainfall received at the Maritime Continent become more pronounced.

Rainfall received across central West Sumatra derives from the Indian Ocean, as both the northern and southern monsoonal trade winds get deflected eastward near equator through Coriolis force. The leeward East of Sumatra, however, is blocked from the humid trade winds by the Barisan mountain range (4) and the Malay Peninsula (Fig. 1*A*). As a result, precipitation is highest in areas West of the mountain range (>3,000 mm/y), and decreases to <2,500 mm/y in the eastern areas (1) (Fig. S2). It further decreases toward the South of Sumatra due to its proximity to the Australian continent.

Lipid Analysis

Lipids were extracted from freeze-dried and finely ground sediment samples (~8 g) using the MARS Xpress microwave extraction system from CEM GmbH. Sediments were suspended in 25 mL of 9:1 dichloromethane (DCM) and methanol (MeOH) and heated to 100 °C for 15 min with stirring. The solvent extract was filtered through a precombusted GF/F filter, then dried at 36 °C under a stream of nitrogen. Total lipid extracts were saponified in 1 M NaOH (aq) at 80 °C for 3 h. Neutral lipids were extracted with hexane, the pH was reduced to ~2 with HCl, and alcanoic (fatty) acids were then extracted into methyl *t*-butyl ether.

To enable analysis by gas chromatography (GC), fatty acids were methylated using BF_3-MeOH (10% wt/wt, Supelco) in DCM (60 °C, 10 min). Fatty acid methyl esters (FAMEs) were then extracted into hexane, dried over Na_2SO_4, and further purified through silica gel column chromatography (hexane/toluene 3:1) and Ag-NO_3-silica gel column chromatography (hexane/DCM 2:1).

The δD values of individual FAMEs were measured at least in duplicate using a Thermo Trace GC^{ULTRA} using He as a carrier gas. The GC was coupled to a Finnigan $Delta^+XP$ isotope ratio mass spectrometer (IRMS) via a pyrolysis furnace operated at 1430 °C. Data processing and the daily H_3^+ correction were accomplished using Isodat v2.5 software as described by Sessions et al. (5). Methane reference gas and a coinjected *n*-C_{36} alkane standard were used for calibration. An external standard consisting of eight fatty acid alkyl esters with known δD values was analyzed periodically to monitor analytical performance and yielded a root-mean-squared accuracy of 4.2‰. We report an average SD of sample *n*-alkanoic acids of about 3.3‰.

The $\delta^{13}C$ values of individual FAMEs were measured in triplicate using a Thermo Scientific Trace GC equipped with a Rxi-5ms column (30 m × 0.25 mm, film thickness 1 μm) coupled to a Delta V^+ IRMS via a combustion furnace operated at 1030 °C. A CO_2 standard gas, together with a coinjected *n*-C_{34} alkane standard, were used for calibration. An external standard of eight fatty acid alkyl esters (the same as used for δD analyses) with known $\delta^{13}C$ values was analyzed periodically to monitor analytical performance. We report an average SD of sample n-alkanoic acids of about 0.6‰.

The δD and $\delta^{13}C$ values were corrected for the isotopic composition of the attached methyl group, which was determined through repeated methylation of a phthalic acid standard of known isotopic composition. We report isotope ratios for the *n*-C_{30} alkanoic acid, which was the most cleanly separated compound of adequate abundance. Additionally, we show δD values for the *n*-C_{32} alkanoic acid for the Holocene period. This restriction derives from poor data quality for the last glacial which is due to both low abundance and coelution of an unknown compound. All δD ($\delta^{13}C$) values are reported as permil [‰] variations relative to the Vienna standard mean ocean water (Vienna Pee Dee Belemnite) standard.

Corrections to the *n*-C_{30} Alkanoic Acid δD Record

The δD record of the *n*-C_{30} alkanoic acid was corrected for glacial–interglacial changes of ice volume and temperature. Correction for changes in ice volume was performed using the $\delta^{18}O_{seawater}$ reconstruction of Shackleton et al. (6). Using the modern Global Meteoric Waterline, changes of $\delta^{18}O_{seawater}$ were multiplied by 8 to approximate corresponding changes of $\delta D_{seawater}$ values, which were subtracted from the *n*-C_{30} alkanoic acid δD record.

Temperature correction (Fig. S3) used a minimum estimate of an LGM to Holocene temperature difference (ΔT) of 3 °C [sea surface temperature off West Sumatra (7, 8)] and a maximum ΔT of 7 °C [West Sumatran highlands (9)]. The effect of ΔT on equilibrium fractionation was approximated as +0.8‰ D per °C [0.1‰ $\delta^{18}O$/°C (10)] and was added to the ice-volume corrected *n*-C_{30} alkanoic acid δD record.

We emphasize that temperature effects other than those on equilibrium fractionation at the evaporating surface, e.g., changes of the atmospheric temperature gradient and raindrop formation temperature, cannot be included at this point. Therefore, the temperature correction suggested here can only be a minimum estimate. Moreover, changes in relative humidity near the evaporative surface and associated kinetic isotope effects cannot be assessed. Given the tropical marine environment of our study site, however, we surmise the impact of kinetic isotope effects during evaporation on our integrated δD record to be small.

Provenance of Sedimentary Long-Chain Alkanoic Acids

Long-chain (>*n*-C_{30}) alkanoic acids recovered from marine sediments have been found to derive almost exclusively from higher terrestrial plants (11). Together with long chain *n*-alkanes and certain alkanols, they are integral parts of higher terrestrial plant leaf waxes (12). Depending on climatic and geomorphic conditions, they may accumulate in the ground (e.g., soils) or be carried by fluvial erosion.

The mineralogy and radiogenic isotope composition of clay minerals in Sumatran Shelf sediments indicate that rocks of North and central Sumatra are the dominant source of terrestrial material (13, 14). According to Ehlert et al. (14), characteristics of local sediment radiogenic isotopes are sharply separated from sediments off central Sumatra, which mix with clays from sources farther south. Our study site is located near the North Sumatran catchment as defined by Ehlert et al. (14) and has been geographically isolated from the southwestern coastline during the

last sea-level lowstand of the LGM through shelf exposure (for a detailed reconstruction of the deglacial shift of coastline position, see refs. 15 and 16). This natural barrier vanished during the Holocene, potentially allowing for mixing of local sediment with laterally advected plant waxes from the Sunda Shelf during sea level rise (15, 16) through concurrent strengthening of the Indonesian Throughflow (17). However, values of alkanoic acid $\delta^{13}C$ remain fairly stable throughout the Holocene. If considerable mixing with sediment from southern sources had occurred, we would expect this to appear as a ^{13}C enrichment, particularly for plant waxes transported from the Australian continent (dominantly C_4 plants). In summary, we therefore infer that higher plant waxes deposited at the study site derive predominantly from the adjacent hinterland of Northwest Sumatra.

Controls of the δD Value of Terrestrial Plant Waxes

Atmospheric Controls. The δD values of higher plant leaf waxes are linked to the isotopic composition of the plant's growth water, i.e., precipitation (18–22). In mid- and low-latitude coastal areas, dominant control on the isotopic composition of rainfall is exerted by the amount of rainfall (23, 24). Here, the degree of reevaporation and condensation during precipitation determines the δD value of rainfall received at the surface (25). This leads to stronger D depletion in areas of high precipitation (and, as a consequence, of high relative humidity) and D enrichment when precipitation and relative humidity are low.

However, whereas δD values of higher plant waxes isolated from marine and lacustrine environments in tropical and subtropical Africa are being interpreted as qualitative estimates of past rainfall amounts (26–29), recent studies indicate that the amount effect alone does not sufficiently explain δD values measured in rainfall across the Maritime Continent (30–33). These studies indicate that δD values of rainwater in equatorial Indonesia are a function of both local rainfall amounts and the rainout history of monsoonally advected moisture from adjacent tropical regions (30, 31). This includes latitudinal transport of air parcels across the Indian Ocean and the Pacific through Walker circulation, which may result in progressive isotope depletion of rainfall with increasing distance from the primary site of evaporation (G. J. Bowen, Gridded maps of the isotopic composition of meteoric precipitation, 2009, available at www.waterisotopes.org). As a result, rainwater δD at a given site may reflect both the amount of local rainfall ("amount effect") as well as the rainout history of the air parcel (30, 31, 33) (see also Bowen online maps, cited above). However, changes of moisture sources resulting from the seasonal migration of the ITCZ do not correspond to a seasonal cycle in rainwater δD collected in NW Sumatra (31), indicating that the amount effect exerts dominant control on the δD value of rainfall in the study area. We therefore interpret changes in alkanoic acid δD to primarily reflect changes in the amount of rainfall across the catchment area of our study site.

Influence of Vegetation. Since there is debate about whether photosynthetic pathway and plant morphology have an influence on the δD value of plant waxes (34), we also measured their $\delta^{13}C$ values during periods of high δD variability to control for changes in photosynthetic pathway (35). Values of $\delta^{13}C$ for the n-C_{30} alkanoic acid from the study site (Fig. 2*C*) show little variation between about −30‰ and −33‰ with slightly more ^{13}C depletion during the LGM. Analyses of air bubbles trapped in an Antarctic ice core (36) indicate that levels of atmospheric ^{13}C during the last glacial were between 0.3‰ and 1‰ lower than during the Holocene. The observed range of 3‰ therefore must partly be attributed to changes in atmospheric $\delta^{13}C$. Palynological studies from the highlands of NW [Lake Toba (37)] and central Sumatra [Danau Padang and Danau di Atas (38, 39)] provide evidence for persistent dominance of tropical trees (C_3 plants) throughout the last 24 ka (summarized in ref. 40). We therefore consider the remaining change of about 2‰ in the n-C_{30} alkanoic acid $\delta^{13}C$ record as too minor to reflect significant changes in the ratio of C_3/C_4 vegetation, the more so as the physiological range in the $\delta^{13}C$ value of tropical tree leaf waxes comprises at least 4‰ (41). We further note that changes other than the ratio of C_3/C_4 plants such as changes of canopy closure may account for considerable variability of $\delta^{13}C$ [about 6‰, canopy effect (42)] among C_3 plants. Our primary conclusion from the carbon isotopic evidence, however, is that we can rule out wholesale ecosystem shifts, and thus hydrogen isotopic variability is likely to reflect hydrological changes. This conclusion is further supported by the rather weak correlation of δD and $\delta^{13}C$ of $r^2 = 0.16$.

1. Fontanel J, Chantefort A (1978) *Bioclimats du monde Indonésien*, ed Legris P [*Bioclimates of the Indonesian Archipelago*]. (Inst Francais Pondichéry, Pondicherry, France). French.
2. Aldrian E, Susanto RD (2003) Identification of three dominant rainfall regions within Indonesia and their relationship to sea surface temperature. *Int J Climatol* 23(12): 1435–1452.
3. Wang B, Ding Q (2008) Global monsoon: Dominant mode of annual variation in the tropics. *Dyn Atmos Oceans* 44(3-4):165–183.
4. Nishimura S, et al. (1984) A gravity and volcanostratigraphic interpretation of the Lake Toba region, North Sumatra, Indonesia. *Tectonophysics* 109(3-4):253–272.
5. Sessions AL, Burgoyne TW, Hayes JM (2001) Correction of H_3^+ contributions in hydrogen isotope ratio monitoring mass spectrometry. *Anal Chem* 73(2):192–199.
6. Shackleton NJ (2000) The 100,000-year ice-Age cycle identified and found to lag temperature, carbon dioxide, and orbital eccentricity. *Science* 289(5486):1897–1902.
7. Lückge A, et al. (2009) Monsoon versus ocean circulation controls on paleoenvironmental conditions off southern Sumatra during the past 300,000 years. *Paleoceanography* 24(1):PA1208, 10.1029/2008PA001627.
8. Mohtadi M, et al. (2010) Late Pleistocene surface and thermocline conditions of the eastern tropical Indian Ocean. *Quat Sci Rev* 29(7-8):887–896.
9. Stuijts I, Newsome JC, Flenley JR (1988) Evidence for late quaternary vegetational change in the Sumatran and Javan highlands. *Rev Palaeobot Palynol* 55(1-3):207–216.
10. Risi C, Bony S, Vimeux F, Jouzel J (2010) Water-stable isotopes in the LMDZ4 general circulation model: Model evaluation for present-day and past climates and applications to climatic interpretations of tropical isotopic records. *J Geophys Res* 115(D12):D12118, 10.1029/2009JD013255.
11. Kusch S, Rethemeyer J, Schefuß E, Mollenhauer G (2010) Controls on the age of vascular plant biomarkers in Black Sea sediments. *Geochim Cosmochim Acta* 74(24): 7031–7047.
12. Eglinton G, Hamilton RJ (1967) Leaf epicuticular waxes. *Science* 156(3780):1322–1335.
13. Gingele FX, De Deckker P, Hillenbrand C-D (2001) Clay mineral distribution in surface sediments between Indonesia and NW Australia — source and transport by ocean currents. *Mar Geol* 179(3-4):135–146.
14. Ehlert C, et al. (2011) Current transport versus continental inputs in the eastern Indian Ocean: Radiogenic isotope signatures of clay size sediments. *Geochem Geophys Geosyst* 12(6):Q06017, 10.1029/2011GC003544.
15. Hanebuth T, Stattegger K, Grootes PM (2000) Rapid flooding of the sunda shelf: A late-glacial sea-level record. *Science* 288(5468):1033–1035.
16. Sathiamurthy E, Voris HK (2006) Maps of Holocene sea level transgression and submerged lakes on the Sunda Shelf. *Nat Hist J Chulalongkorn Univ* (Suppl. 2): 1–44.
17. Linsley BK, Rosenthal Y, Oppo DW (2010) Holocene evolution of the Indonesian throughflow and the western Pacific warm pool. *Nat Geosci* 3(8):578–583.
18. Sessions AL, Burgoyne TW, Schimmelmann A, Hayes JM (1999) Fractionation of hydrogen isotopes in lipid biosynthesis. *Org Geochem* 30(9):1193–1200.
19. Chikaraishi Y, Naraoka H (2003) Compound-specific δD-$\delta^{13}C$ analyses of *n*-alkanes extracted from terrestrial and aquatic plants. *Phytochemistry* 63(3):361–371.
20. Sachse D, Radke J, Gleixner G (2004) Hydrogen isotope ratios of recent lacustrine sedimentary n-alkanes record modern climate variability. *Geochim Cosmochim Acta* 68(23):4877–4889.
21. Sachse D, Radke J, Gleixner G (2006) δD values of individual n-alkanes from terrestrial plants along a climatic gradient—Implications for the sedimentary biomarker record. *Org Geochem* 37(4):469–483.
22. Hou J, D'Andrea WJ, Huang Y (2008) Can sedimentary leaf waxes record D/H ratios of continental precipitation? Field, model, and experimental assessments. *Geochim Cosmochim Acta* 72(14):3503–3517.
23. Dansgaard W (1964) Stable isotopes in precipitation. *Tellus* 16(4):436–468.
24. Rozanski K, Araguas-Araguas L, Gonfiantini R (1993) Isotopic patterns in modern global precipitation. *Climate Change in Continental Isotopic Records*, Geophysical Monograph Series, eds Swart PK, Lohmann KC, McKenzie J, Savin S (Am Geophys Union, Washington, DC), Vol 78, pp 1–36.
25. Worden J, Noone D, Bowman K; Tropospheric Emission Spectrometer Science Team and Data contributors (2007) Importance of rain evaporation and continental convection in the tropical water cycle. *Nature* 445(7127):528–532.

26. Schefuss E, Schouten S, Schneider RR (2005) Climatic controls on central African hydrology during the past 20,000 years. *Nature* 437(7061):1003–1006.
27. Tierney JE, et al. (2008) Northern Hemisphere controls on tropical southeast African climate during the past 60,000 years. *Science* 322(5899):252–255.
28. Niedermeyer EM, et al. (2010) Orbital- and millennial-scale changes in the hydrologic cycle and vegetation in the western African Sahel: Insights from individual plant wax δD and $\delta^{13}C$. *Quat Sci Rev* 29(23-24):2996–3005.
29. Schefuss E, Kuhlmann H, Mollenhauer G, Prange M, Pätzold J (2011) Forcing of wet phases in southeast Africa over the past 17,000 years. *Nature* 480(7378): 509–512.
30. Cobb KM, Adkins JF, Partin JW, Clark B (2007) Regional-scale climate influences on temporal variations of rainwater and cave dripwater oxygen isotopes in northern Borneo. *Earth Planet Sci Lett* 263(3-4):207–220.
31. Kurita N, Ichiyanagi K, Matsumoto J, Yamanaka MD, Ohata T (2009) The relationship between the isotopic content of precipitation and the precipitation amount in tropical regions. *J Geochem Explor* 102(3):113–122.
32. Breitenbach SFM, et al. (2010) Strong influence of water vapor source dynamics on stable isotopes in precipitation observed in Southern Meghalaya, NE India. *Earth Planet Sci Lett* 292(1-2):212–220.
33. Dayem KE, Molnar P, Battisti DS, Roe GH (2010) Lessons learned from oxygen isotopes in modern precipitation applied to interpretation of speleothem records of paleoclimate from eastern Asia. *Earth Planet Sci Lett* 295(1-2):219–230.
34. Smith FA, Freeman KH (2006) Influence of physiology and climate on δD of leaf wax *n*-alkanes from C_3 and C_4 grasses. *Geochim Cosmochim Acta* 70(5):1172–1187.
35. O'Leary MH (1981) Carbon isotopic fractionation in plants. *Phytochemistry* 20(4):553–567.
36. Leuenberger M, Siegenthaler U, Langway C (1992) Carbon isotope composition of atmospheric CO_2 during the last ice age from an Antarctic ice core. *Nature* 357(6378): 488–490.
37. Maloney BK (1980) Pollen analytical evidence for early forest clearance in North Sumatra. *Nature* 287(5780):324–326.
38. Morley RJ (1982) A palaeoecological interpretation of a 10,000 year pollen record from Danau Padang, Central Sumatra, Indonesia. *J Biogeogr* 9(2):151–190.
39. Newsome J, Flenley JR (1988) Late Quaternary vegetational history of the central highlands of Sumatra. II. Palaeopalynology and vegetational history. *J Biogeogr* 15(4): 555–578.
40. van der Kaars S, Bassinot F, De Deckker P, Guichard F (2010) Changes in monsoon and ocean circulation and the vegetation cover of southwest Sumatra through the last 83,000 years: The record from marine core BAR94-42. *Palaeogeogr Palaeoclimatol Palaeoecol* 296(1-2):52–78.
41. Vogts A, Moossen H, Rommerskirchen F, Rullkötter J (2009) Distribution patterns and stable carbon isotopic composition of alkanes and alkan-1-ols from plant waxes of African rain forest and savanna C3 species. *Org Geochem* 40(10):1037–1054.
42. van der Merwe NJ, Medina E (1991) The canopy effect, carbon isotope ratios and foodwebs in Amazonia. *J Archaeol Sci* 18(3):249–259.

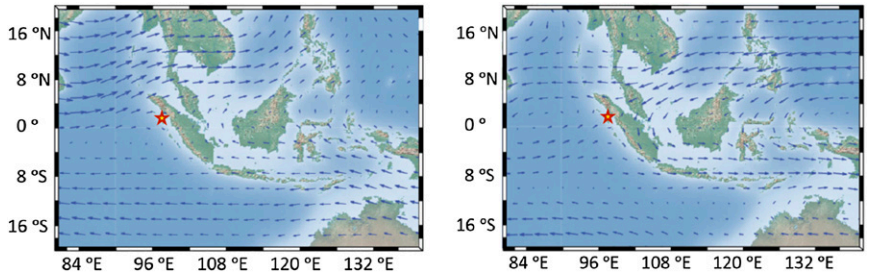

Fig. S1. Seasonal cyclicity of the Northwest and Southwest monsoons. Arrows indicate wind vectors at 850 mbar during (*Left*) the summer (JJA) and (*Right*) the winter (JFM) season averaged from 1945 to 2010 (NCEP Reanalysis 2 data, provided by NOAA/OAR/ESRL PSD, available at www.esrl.noaa.gov/psd/). Star indicates the position of the study site.

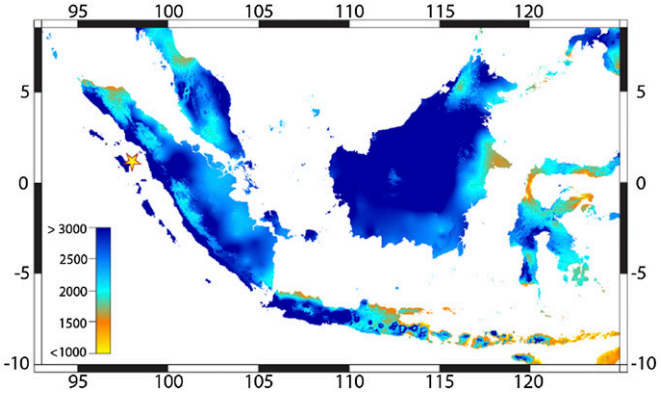

Fig. S2. Mean annual precipitation across the Maritime Continent. Color coding indicates annual mean precipitation (mm y^{-1}) received at the Maritime Continent averaged from 1950 to 2000, available at www.worldclim.org/. Yellow star indicates the location of the study site.

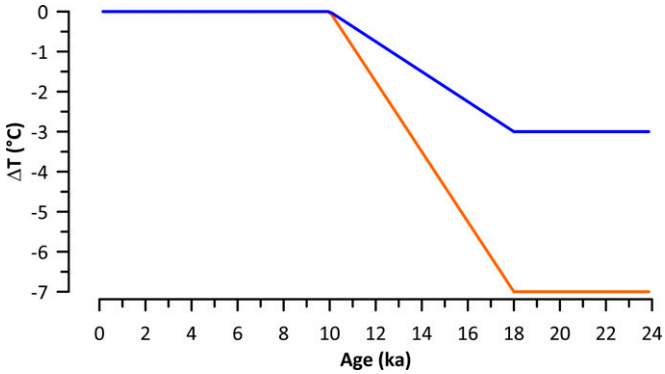

Fig. S3. Temperature functions applied for the correction of the *n*-C_{30} alkanoic acid δD record. Blue (orange) line depicts a deglacial warming of 3 °C (7 °C).

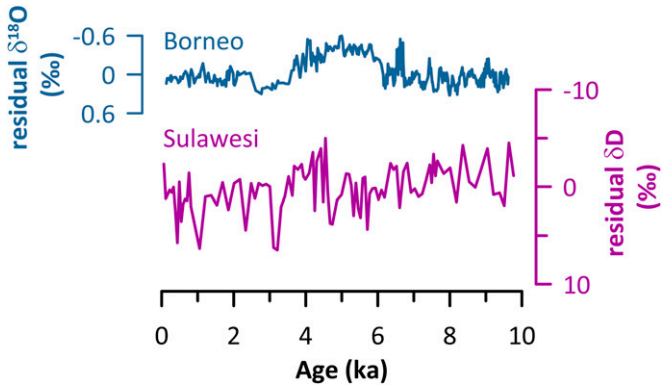

Fig. S4. Residual isotope records from Borneo (1) and Sulawesi (2) after detrending (3) to reveal precipitation changes on central Indo-Pacific Warm Pool rainfall other than those induced by sea level rise.

1. Partin JW, Cobb KM, Adkins JF, Clark B, Fernandez DP (2007) Millennial-scale trends in west Pacific warm pool hydrology since the Last Glacial Maximum. *Nature* 449(7161):452–455.
2. Tierney JE, et al. (2012) The influence of Indian Ocean atmospheric circulation on Warm Pool hydroclimate during the Holocene epoch. *J Geophys Res* 117(D19):D19108, 10.1029/2012JD018060.
3. Rybicki GB, Press WH (1995) Class of fast methods for processing irregularly sampled or otherwise inhomogeneous one-dimensional data. *Phys Rev Lett* 74(7):1060–1063.